Comparison of Combustion Experiments and Theory in Polyethylene Solid Fuel Ramjets

P. J. M. Elands,* P. A. O. G. Korting,† and T. Wijchers‡
Prins Maurits Laboratory TNO, Rijswijk, the Netherlands
and
F. Dijkstra§
Delft University of Technology, Delft, the Netherlands

A research program was carried out to validate numerical simulation of the flow and combustion processes in the combustion chamber of a solid fuel ramjet with experimental results. Experimental data were obtained by burning cylindrical fuel grains made of polyethylene in a solid fuel ramjet using a connected pipe facility. For numerical simulation a computer code describing two-dimensional, steady-state turbulent flows through channels with and without a sudden expansion was developed. Three different combustion models are incorporated, one based on finite-rate chemical kinetics, the other two based on the diffusion flame concept. For the validation, emphasis was laid on comparing regression rate data in relation to chamber pressure, air mass flow, inlet air temperature, and step height. Attention was also paid to reattachment length, temperature, and C_2 and CH concentrations. In some cases, a comparison with findings from other investigators was also made. The results show good agreement between predicted and observed behavior downstream of the recirculation zone. In the recirculation zone, however, the agreement is rather poor and can be attributed to the inability of the k-ϵ model to predict heat transfer behind a rearward facing step accurately. It is shown that the effective heat of gasification of the fuel is an important parameter. A better understanding of its behavior in relation to combustion chamber conditions is needed. Computed regression rate data are relatively insensitive to the combustion model employed.

Nomenclature

c_p = specific heat at constant pressure
d = diameter
f = mixture fraction
g = variance of mixture fraction
h = specific enthalpy
h_v = effective heat of gasification
k = turbulent kinetic energy
L = length
M = molar mass
m = mass flow rate
p = static pressure
q = heat flux
R = radius
R_0 = universal gas constant
r = regression rate
S = source term
T = temperature
t = time
u = velocity in x direction
v = velocity in y direction
x = coordinate
Y = mass fraction
y = coordinate
Γ = diffusion coefficient
ϵ = dissipation rate of turbulent kinetic energy
ϕ = arbitrary independent variable
ρ = density

Subscripts
c = chamber
in = inlet
j = Euler index
p = port
r = reattachment
s = species
w = wall
0 = initial or reference

Superscripts
$-$ = mean
$\cdot$ = rate
0 = reference

Presented as Paper 88-3043 at the AIAA/ASME/ASEE/SAE 24th Joint Propulsion Conference, Boston, MA, July 11-13, 1988; received Aug. 31, 1988; revision received Aug. 10, 1989.

*Scientist.
†Head, Rocket Propulsion Section. Member AIAA.
‡Senior Scientist; work conducted while with the Faculty of Aerospace Engineering, Delft University of Technology.
§Research Assistant, Faculty of Aerospace Engineering.

Introduction

In a solid fuel ramjet (SFRJ), air is fed into the bore of a solid fuel grain (see Fig. 1). A diaphragm is used to create a sudden expansion. Behind this sudden expansion, a recirculation zone acts as a flame stabilizer. At the interface between the pyrolyzing fuel and the air, combustion takes place.

At the Prins Maurits Laboratory TNO and the Faculty of Aerospace Engineering of the Delft University of Technology both experimental[1-6] and theoretical[7-11] work has been carried out to investigate the flow and combustion processes in an

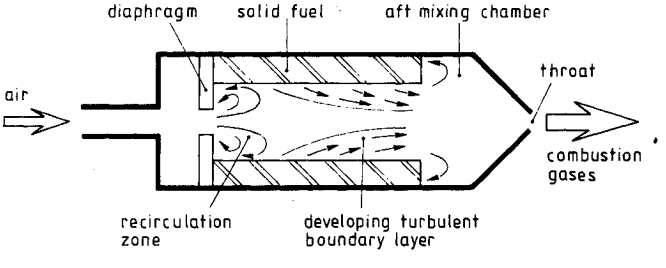

Fig. 1 Schematic view on a solid fuel ramjet combustion chamber.

SFRJ. Other research on solid fuel ramjet combustion has been carried out by, for instance, the Naval Postgraduate School in the United States,[12-14] Technion in Israel,[15-16] and the German Aerospace Research Establishment (DLR) in Germany.[17,18] Technion and DLR mainly have been focusing their attention on experimental work, whereas the Naval Postgraduate School has been carrying out both theoretical and experimental work.

The aim of the present study was to validate the computer code COPPEF[7] (Computer Program for Parabolic and Elliptic Flows) by comparing computational and experimental results. It was not possible to obtain sufficient experimental data from other investigators, which could be used for comparison, mostly due to unknown conditions and assumptions made by these investigators. Furthermore, the COPPEF computer code is not able to handle certain conditions or geometries, e.g., side-dump combustors. Therefore, it was decided to perform a number of experiments to provide additional experimental data. Where possible, however, results from other investigators were used.

One of the combustion models in the COPPEF code is based on finite-rate chemical kinetics and can handle only simple hydrocarbons. For this reason polyethylene (PE) was selected as a fuel for this study. As radiative heat transfer is not yet implemented in this code, the experiments were carried out at pressures below 0.6 MPa, where soot formation is known to be low,[1] and hence radiation is of less importance. The regression rate plays an important role in the performance of an SFRJ. Since it appears to be relatively constant during combustion, the regression rate was chosen to be the prime parameter upon which validation is based. Therefore, the dependency of the regression rate on chamber pressure, air mass flow, inlet air temperature, and step height has been investigated numerically and experimentally. In a number of cases, this validation could be extended also to parameters such as reattachment lengths, temperatures, and concentrations of the C_2 and CH radicals.

Theoretical Modeling

To describe the flow and combustion processes in an SFRJ, a computer program, COPPEF, was developed.[7] This program calculates two-dimensional, steady-state turbulent flows through pipes, with or without a sudden expansion, or through a single-sided sudden expansion configuration. Turbulence is accounted for by Favre averaging of the conservation equations and by modeling terms containing products of fluctuating variables with the high Reynolds number version of the k-ϵ turbulence closure model. All of the governing equations can be cast in the following general form:

$$\frac{\partial}{\partial x_j}(\rho u_j \phi) - \frac{\partial}{\partial x_j}\left(\Gamma_\phi \frac{\partial \phi}{\partial x_j}\right) = S_\phi \tag{1}$$

where ϕ can be u, v, p, k, ϵ, h, f, g, or Y_s. The enthalpy h is defined as

$$h = \sum_s Y_s h_s \tag{2}$$

where Y_s is the mass fraction of species s and

$$h_s = h_s^0(T_0) + \int_{T_0}^{T} c_{p_s}\, dT \tag{3}$$

The equation of state is written as

$$p = \rho R_0 T \sum_s Y_s / M_s \tag{4}$$

The influence of density gradients on the turbulence field is taken into account by a special pressure-velocity correlation term occurring in the equations for k and ϵ.[7]

At the inlet of the SFRJ combustion chamber, the values of all variables are specified. At the outlet and at the center line a zero-gradient condition is specified for all variables, except for the radial velocity which is zero. At the solid wall, the temperature, the mass fractions, and both velocities are specified. The values of k and ϵ are not specified at the wall but are calculated just near the wall using the wall-function method of Chieng and Launder.[19] This two-layer wall-function method is adapted in the case of a small nonzero normal velocity at the wall. Heat transfer at the boundaries is taken into account by coupling the heat flux to the wall to the near-wall variation of the temperature. Mass transfer at the boundaries is included by the injection of gaseous ethylene at the solid wall. The injection velocity is a function of the heat flux.

Three combustion models have been implemented in the COPPEF computer program. Two models, the diffusion flame models, are based on the assumption that the combustion process can be described by one irreversible infinitely fast chemical reaction (mixed is burnt).[8] In one of these two models, the mass fractions are weighted with the β probability density function (pdf) to take into account the effect of turbulence on the combustion process. Both models require the solution of a transport equation for the mixture fraction f, whereas for the β pdf model, the variance of f, called g, must also be calculated. The third model is based on finite-rate chemical kinetics and involves a large number of species and reactions. Dissociation and formation of intermediates is included. The effect of turbulence on the combustion process is neglected.

A finite-volume integration method is employed to reduce the system of partial differential equations describing the flow to a system of algebraic difference equations which can be solved numerically. The combined convective-diffusive fluxes at the cell interfaces are approximated with the power-law scheme.[20] The solution is carried out in a segregated approach, in which an iteration procedure takes into account the nonlinear coupling between the equations. The strong coupling between the pressure and the velocity field is handled by the SIMPLER[20] (Semi-Implicit Method for Pressure-Linked Equations Revised) algorithm together with a line continuity and a block correction procedure.

Experimental Setup

A schematic view of the main parts of the connected pipe facility is given in Fig. 2. A computer-operated gas supply system[2] (not shown in the figure) supplies air, oxygen, hydrogen, nitrogen, and methane. Mass flows are controlled by sonic control and measuring chokes (SCMCs)[3] with an accuracy of about 1.5%. In the vitiator, methane is burnt with oxygen to raise the SFRJ inlet air temperature, and the oxygen content in this heated air is kept constant to that of ambient air.

Before an actual experiment could take place, the air was first vented into the atmosphere by a shuttle valve. As soon as

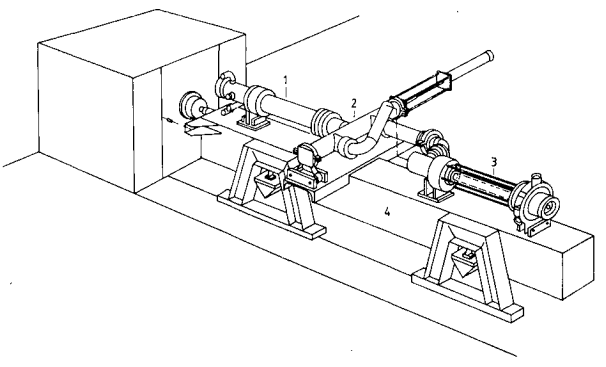

Fig. 2 Experimental setup without spectroscopic equipment: 1) vitiator, 2) shuttle valve, 3) solid fuel ramjet combustion chamber, and 4) thrust bench.

the flow and combustion in the vitiator achieved steady-state conditions, the shuttle valve was opened towards the SFRJ. Simultaneously, oxygen and hydrogen were injected during 2–4 s in the SFRJ-injection chamber (see Fig. 2) and ignited by a spark plug. The hot oxygen-hydrogen flame on its turn ignited the solid fuel grain.

An aft mixing chamber was used to increase the combustion efficiency. The length of the aft mixing chamber could be varied. By adjusting the throat diameter of the nozzle in the aft mixing chamber, the chamber pressure was also varied. Fuel grains can be varied up to 190 mm o.d. and 1000 mm length. The SFRJ, the vitiator, and the shuttle valve were mounted on a thrust bench. Data were recorded on ultraviolet (uv) recorders, magnetic tape, and floppy disks.

To determine the instantaneous local regression rate, an ultrasonic pulse echo technique was employed.[4] A sound pulse generated by an ultrasonoscope is reflected at the interface between two media, e.g., at the regressing solid-gas interface of the fuel and received again. An ultrasonic regression rate analyzer (URRA) determines the time lapse between the emitted and the received pulse. If the velocity of sound is known, the momentary wall thickness and, hence, the regression rate can be determined.

Although polyethylene (PE) diffuses light, it is spectroscopically almost uniformly transparent. Therefore, spectroscopy and pyrometry were used as nonintrusive diagnostic techniques. Radiation from the combustion gases through the solid fuel wall was transmitted via a set of lenses and mirrors into a spectrograph. The spectrograph was equipped with a 25-mm-long, 1000-channel, intensified diode array detector. From the spectra obtained, temperatures and species concentrations were determined. More details are given by Wijchers.[5]

Soot temperatures were determined with the aid of a pyrometer, which measures the ratio of the spectral radiances at 577 and 830 nm. The difference between this temperature and the temperature of the soot among the gas is assumed to be negligible. Furthermore, soot is assumed to be a grey radiator. A description of the pyrometer can be found in Ref. 6.

Results and Discussion

The computer code assumes a steady-state flow and combustion process. This assumption is in strong contrast with the actual situation, where, due to a regular vortex shedding at the inlet, locally highly fluctuating quantities such as velocities, temperatures, and species concentrations can be expected. Nevertheless, a relatively constant regression rate during the combustion of PE with air is observed, as shown in Fig. 3. For this study, however, regression rates were obtained from weight loss measurements.

For this comparison study, a set of standard conditions was defined for both the experimental setup and the computational model. These conditions are specified in Table 1. Unless stated otherwise, the results refer to these standard conditions. To investigate the effect of chamber pressure, air mass flow, inlet air temperature, and step height on regression rate, each of these parameters was varied while the others were kept constant. In the following some comments are made on the way this comparison study was carried out.

First, in the computer code, the local regression rate is modeled as follows[9]:

$$r = \frac{q_w}{\rho_w h_v} \tag{5}$$

where h_v is defined as the amount of heat required to pyrolyze 1 kg of fuel. Values found for h_v in the literature range from 1.7–6 MJ/kg and depend on the heat transfer mechanism.[21-23] For convective heat transfer, values between 4.0 and 5.5 MJ/kg are often encountered for PE.[10] Figure 4 shows the effect of variation of h_v on predicted regression rates and a comparison with experimental results. A low effective heat of gasification not only predicts a much higher regression rate, but also a much stronger dependency on mass flow, compared to higher values for h_v. This emphasizes the importance of a correct value for the effective heat of gasification to predict the regression rate properly. Although the wall temperature, the effective heat of gasification, and the fuel composition will vary with time and location, these parameters have been kept constant since little knowledge on their behavior presently exists. For this study a value of 4 MJ/kg was assumed.

Second, in the computer code, the regression rate is also determined by convective heat transfer from the main flow to the wall and is therefore related to the near-wall temperature gradient. Although the flame temperatures predicted by the various combustion models may differ significantly, the near-wall temperature gradient is not affected very much. It should be noted that the wall temperature is kept constant and uniform at these calculations. This results in similar predictions for the regression rate using the different combustion models

Table 1 Standard conditions for experimental setup and computational model

	Experiments	Theory
Oxidizer	Air	Air
Fuel	Polyethylene	Monomer C_2H_4
m_{air}	150 g/s	150 g/s
T_{in}	300 K	300 K
L	300 mm	300 mm
d_{in}	15 mm	15 mm
d_{p_0}	40 mm	——
d_p	——	45 mm
p_c	0.3–0.5 MPa	0.45 MPa
h_v	——	4 MJ/kg
T_{wall}	——	800 K
		Diffusion flame module
		20 × 20 grid
Inlet velocity profile		Uniform
Inlet turbulence level		$k_{in} = 0.5 \cdot (0.1 \cdot u_{in})^2$
Ultrasonics	250 mm from inlet	
Spectroscopy	265 mm from inlet	
Pyrometry	Scanning along grain axis	

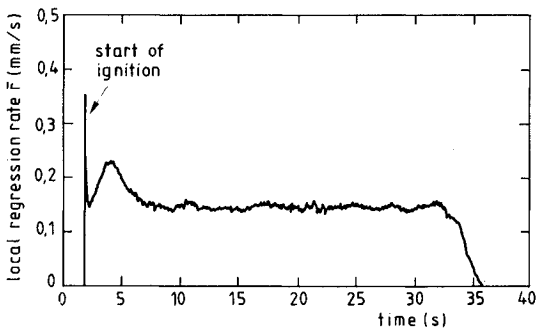

Fig. 3 Local regression rate behavior of PE vs time.

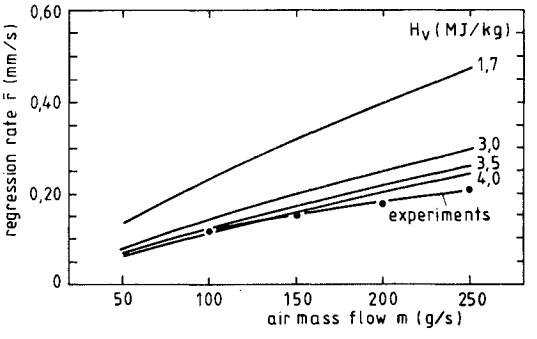

Fig. 4 Comparison of calculated and experimental regression rates for different effective heats of gasification.

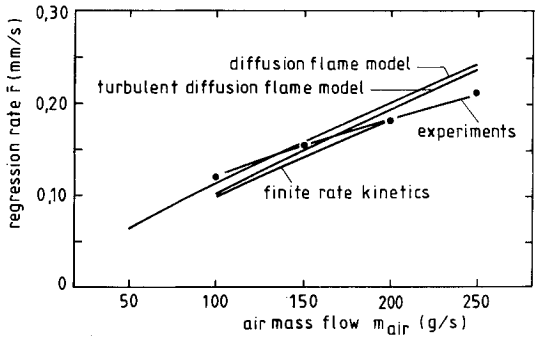

Fig. 5 Comparison between calculated regression rate data for three different combustion models with experimental data.

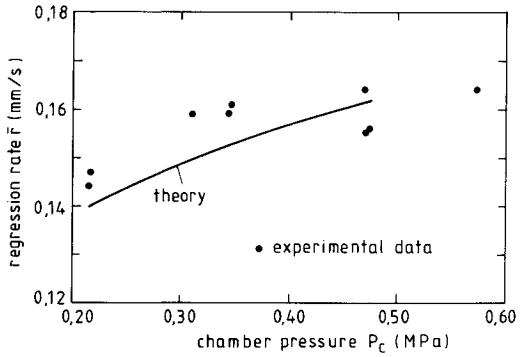

Fig. 6 Calculated and experimental regression rate data as a function of chamber pressure.

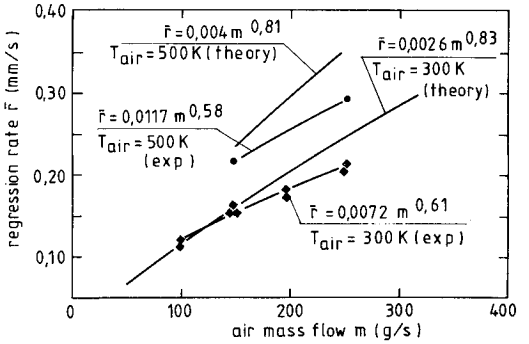

Fig. 7 Calculated and experimental regression rate data in relation to air mass flow rate at two different inlet air temperatures.

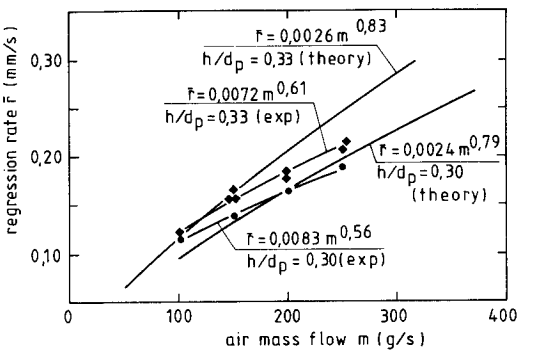

Fig. 8 Effect of air mass flow rate on calculated and experimental regression rates.

(see Fig. 5). For regression rate predictions, therefore, calculations were conducted using the diffusion flame model and occasionally checked using the other models. The mean regression rate is obtained by averaging the predicted local regression rates.

Third, parameters such as reattachment length and peak regression rate location depend on inlet conditions, in particular turbulence levels.[24,25] Because inlet conditions were not determined experimentally, the inlet velocity was assumed to be distributed uniformly over the inlet area in the calculations. The turbulence intensity was chosen to be 0.1, according to Vos[7]; see Table 1.

Finally, during an experiment, the diameter of the inner bore of the fuel grain, and hence the step height, increases with time. Because the regression rate reaches its steady-state value after about 5 s, the corresponding step height will be larger. For computer simulation, the initial grain diameter was chosen to be 45 mm instead of the initial grain diameter of 40 mm at the experiments. This corresponds with the time- and location-averaged, inner grain diameter during combustion for the majority of the experiments.

Mean Regression Rate

In Fig. 6, the mean regression rate is given as a function of the chamber pressure p_c. As mentioned, the chamber pressures were kept relatively low to avoid soot formation and hence to minimize radiative heat transfer. The calculations show a slight dependency of the mean regression rate on the chamber pressure, and the experiments show hardly any dependency as was expected at these low pressures.[1] Also at other conditions the effect of pressure on the regression rate appears to be small both in the experiments and in the calculations.

In Fig. 7, the mean regression rate is given as a function of the inlet air mass flow for two inlet air temperatures. From this figure, it is observed that the predicted dependency of the regression rate on the air mass flow is stronger than for the experimental one. This difference also increases with increasing inlet air temperature. From the calculations, the exponent of the mass flow appears to be about 0.8, which would be expected if only convective heat transfer is considered.[26] The experimental exponent is somewhat lower indicating that also other regression rate determining mechanisms are involved.

A closer examination of the regression rate behavior reveals that this difference is especially apparent in the recirculation region. This is possibly due to the inability of the k-ϵ turbulence closure model, in combination with wall functions, to predict the heat transfer behind a step accurately.[27] At relatively low Reynolds numbers ($< 2 \cdot 10^5$, based on the inlet velocity and on the fuel port diameter), the heat transfer is likely to be underpredicted, whereas at higher Reynolds numbers, the heat transfer is overpredicted. At higher mass flow rates, Reynolds numbers are high ($> 5 \cdot 10^5$), and therefore regression rates will be overpredicted in the recirculation region. In Ref. 27 an adaptation of the Chieng and Launder wall-function method is proposed to improve heat transfer prediction, changing the power dependence on Re from about 0.8 to 0.66. Similar deficiencies of the k-ϵ model, especially with respect to the value of ϵ at the step face, were noticed by Launder and Spalding,[24] Milshtein and Netzer,[12] Stevenson and Netzer,[13] and Netzer.[14]

The same effect is also noticed if the mean regression rate is considered as a function of the air mass flow at two different step height to diameter ratios (see Fig. 8).

In Fig. 9, the effect of step height is shown at two different air inlet temperatures. Especially the combination of a high inlet air temperature and a high ratio of step height to diameter yields larger differences between the predicted and observed regression rates. Apparently by raising the inlet air temperature and step height, the inability of the k-ϵ model to follow the increased heat transfer becomes more pronounced.

The observed differences, however, may not only be caused by an improper heat transfer prediction by the k-ϵ model but may also be attributed to a change in effective heat of gasification. It is most likely[10] that the effective heat of gasification is affected by parameters such as near-wall temperature, flow velocity, and fuel decomposition temperature. Therefore, it

may not be constant from one set of conditions to another and may also vary along the fuel grain. These effects, however, have yet to be incorporated in the computer code.

The mean regression rate as a function of the inlet air temperature at two different step height to diameter ratios is given in Fig. 10. The predicted results agree fairly well with experimental data. In Fig. 11, the effect of inlet air temperature on mean regression rate is given at two different mass flows. From this figure, the discrepancy between calculated and measured data at higher mass flows is clearly seen and again may be attributed to the k-ϵ model being unable to follow the observed increased heat transfer.

Local Mean Regression Rate

The experimental regression rate, as discussed previously, was obtained by weight loss measurements. Local mean regression rates have been obtained by measuring the inner grain profile after combustion. In both cases, however, the regression rate is not only determined by the combustion process itself, but also to some extent by the ignition. During ignition, a relatively large fuel regression is observed (see Fig. 3), especially close to the inlet. This regression influences the final inner grain profile. This behavior can only be reduced, but never eliminated, by long burning times. The regression rate data were not corrected for this ignition phase. Therefore, after correction, local mean regression rates would be somewhat lower, particularly in the recirculation region. Highest regression rates normally occur at the end of the recirculation zone and are assumed to correspond with the so-called reattachment point.

Figures 12–14 compare the calculated and experimentally observed local mean regression rates along the fuel grain. In these figures, the results at standard conditions are given, while in addition the results obtained after varying the step height, the inlet air temperature, and the mass flow, respectively, are plotted. It can be concluded that the local mean regression rate downstream of the recirculation zone is predicted rather well. However, as far as the recirculation zone itself is concerned, generally a large discrepancy exists between calculated and experimental results. This result confirms the

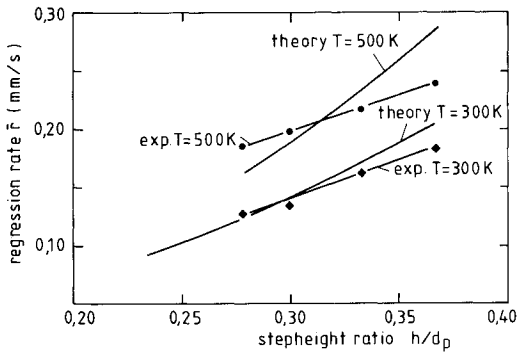

Fig. 9 Calculated and experimental regression rates vs step-height ratio.

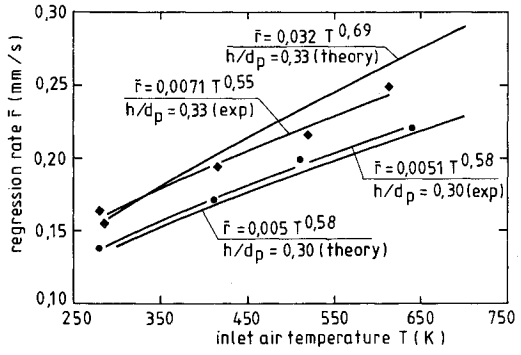

Fig. 10 Calculated and experimental regression rate vs inlet air temperature.

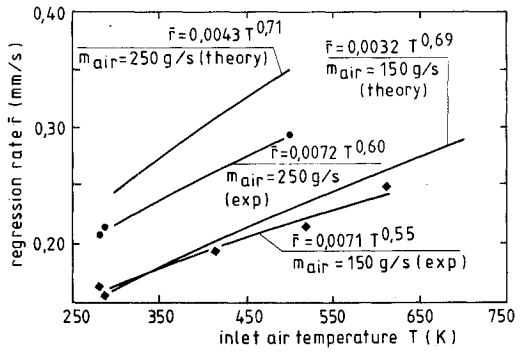

Fig. 11 Calculated and experimental regression rate vs inlet air temperature and air mass flow rate.

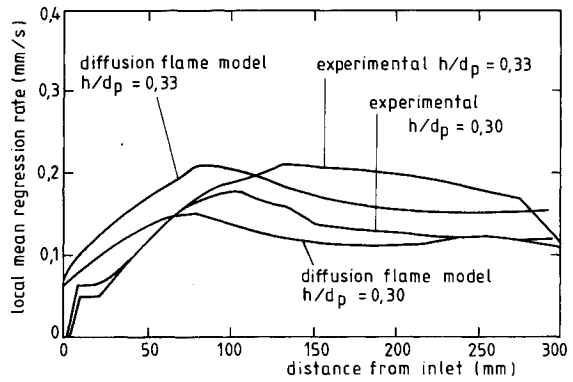

Fig. 12 Calculated and observed local mean regression rates at two different step-height ratios.

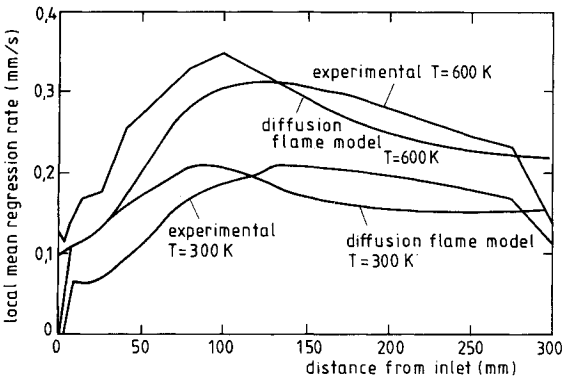

Fig. 13 Calculated and observed local mean regression rates at two different inlet air temperatures.

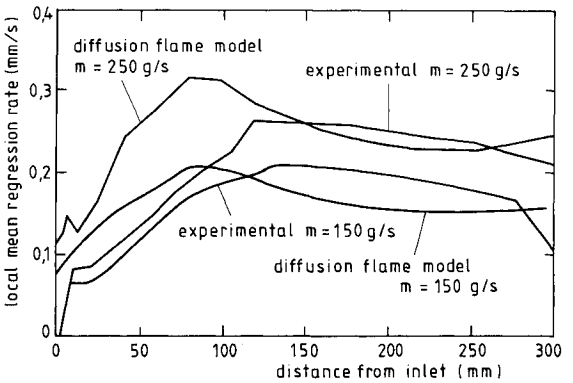

Fig. 14 Calculated and observed local mean regression rate at two different air mass flow rates.

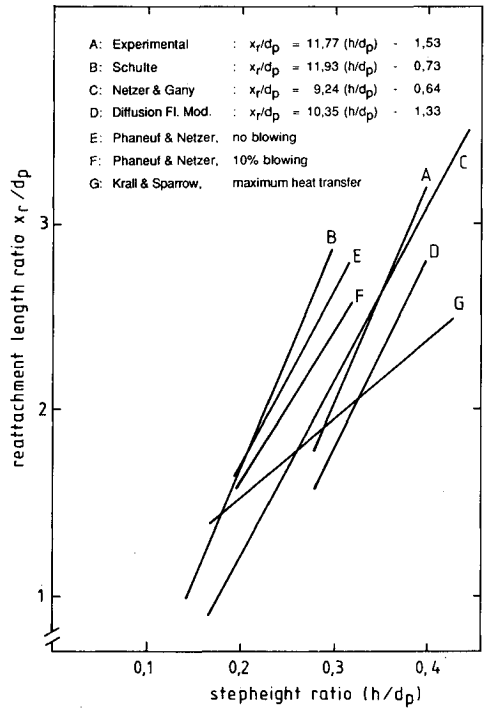

Fig. 15 Reattachment length ratio vs step-height ratio.

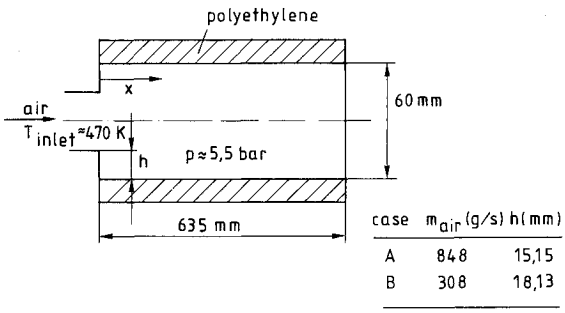

Fig. 16 Experimental conditions and dimensions of the fuel grain.

shortcomings of the k-ϵ model, as stated above. The predictions only seem to improve when the conditions are less sensitive to the turbulence predictions, i.e., at lower step height.

Recirculation Zone

The location of the reattachment point depends primarily on step height. For a number of experiments, this point was determined by assuming that its location corresponds to the position of the maximum local mean regression rate. In Fig. 15, the experimental reattachment points are plotted vs step height and show good agreement with predicted values. The predicted reattachment lengths were obtained by extrapolating the zero-velocity line and are influenced by the k-ϵ model and the inlet turbulence level.[25]

In addition, experimental and predicted results obtained by Schulte et al.,[17] Netzer and Gany,[15] Phaneuf and Netzer,[28] and Krall and Sparrow[29] are included in this figure. The data of Schulte et al. are based on the markings of the flow pattern on the PE surface after a test run. Because of this different approach, only the slope of the linear curve-fit of the DLR results can be compared with the results of this study. Here, good agreement is achieved, too. In fact, all lines, except the line for the experiment of Krall and Sparrow, lie in a reasonable range and have more or less the same slope.

Radial Temperature Profiles

Detailed radial temperature measurements were not performed during the present experimental test runs. Schulte et al.,[18] however, have measured temperature profiles in a similar experimental setup also utilizing PE as a fuel. Two of their test conditions were selected for comparison with computational results. In the following discussions, these test conditions will be denoted as A and B. These conditions and the dimensions of the fuel grain are given in Fig. 16. Temperature profiles were measured using a platinum/rhodium thermocouple, which was moved through the fuel grain into the combustor

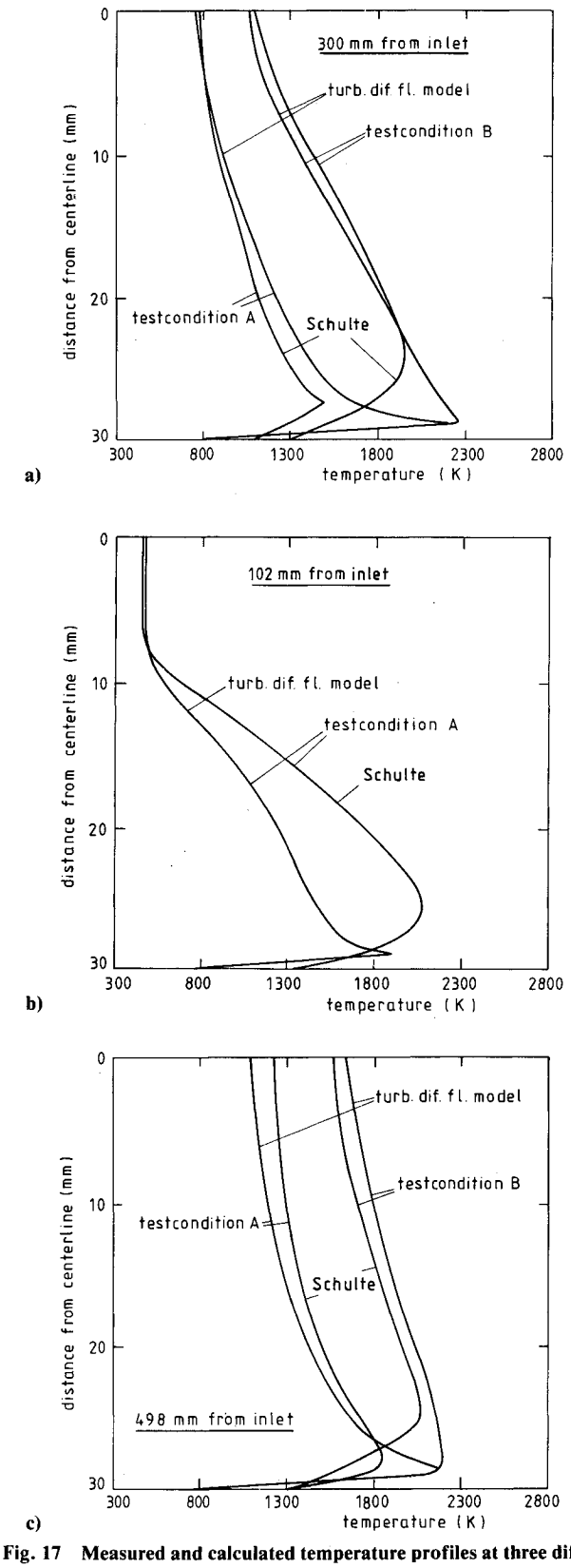

Fig. 17 Measured and calculated temperature profiles at three different x locations along the grain.

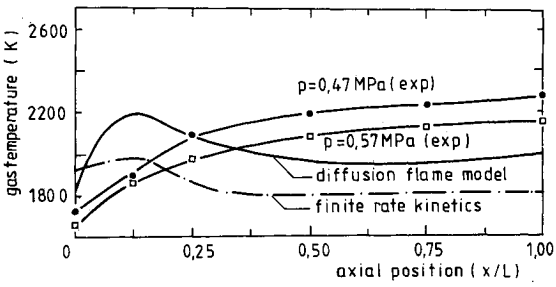

Fig. 18 Maximum gas temperatures along the fuel grain.

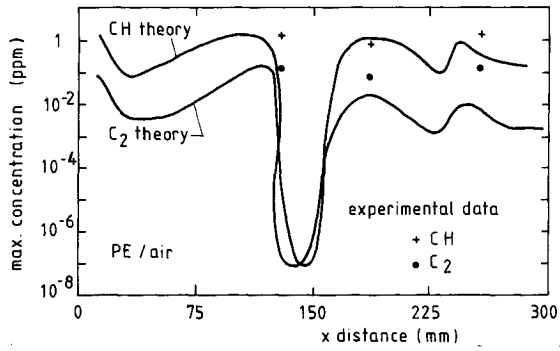

Fig. 19 Maximum concentrations of C_2 and CH radicals along the fuel grain.

with the aid of a motor drive. Corrections were made for radiation effects. For test condition A, a large mass flow was employed. Since the computer code is known to overpredict regression rates at such large mass flows, it was decided to prescribe a regression rate leading to a similar equivalence ratio as the one measured by Schulte et al.[18] For test condition B, however, the regression rate was predicted by the computer code. Here, the predicted equivalence ratio corresponded well with the experimentally observed ratio. In both cases, the turbulent diffusion flame combustion model was employed. In Figs. 17a–17c, the experimental and computational results are compared at three different locations along the fuel grain: near the entrance (recirculation zone), halfway along the grain, and near the end, respectively. Figure 17a shows clearly the large discrepancy between predicted and measured temperature profiles. This discrepancy again is attributed to the inability of the k-ϵ model to predict heat transfer behind a rearward facing step accurately. Figures 17b and 17c, however, show a good correlation, except for the temperatures in the flame sheet region. In that region, the predicted temperatures are much higher than the measured values. Although the turbulent diffusion flame model is expected to predict maximum temperatures that generally will be too high because species dissociation is not considered, this omission cannot fully explain the large differences encountered here.

Axial Temperature Profiles

For a number of test conditions, maximum temperatures have been determined as a function of axial position by means of a pyrometer. This pyrometer measures the so-called color temperature,[6] which in the case of a grey body, is equal to the actual temperature of this body. Because some soot is always present in the combustion chamber, and soot is assumed to be a grey body, the color temperature of the soot may be considered as the gas temperature.

In Fig. 18, the maximum gas temperature in every port cross section along the fuel grain is shown for two different chamber pressures. A temperature increase with axial position is observed. There is a relation between pressure and maximum observed temperature at these pressures. This cannot be explained by soot formation alone, which indeed gradually increases with increasing pressure. In this pressure region, however, soot formation is still poor, and the regression rate is not affected by soot radiation.[1] Apparently other yet unknown mechanisms are responsible for this behavior.

In Fig. 18, the computational results are also shown for both the diffusion flame model and the finite-rate chemical kinetics model. The results apply for pressures of 0.47 and 0.57 MPa. The differences between the results from the two models can be attributed to the diffusion flame model, which ignores dissociation. Since a temperature peak is calculated in the recirculation zone, the computed behavior is different from the experimental behavior. Downstream of the recirculation zone the prediction is more in agreement with the experimental data obtained at higher pressures.

Radical Species

The spectroscopic equipment employed is capable of recording spectra with a bandwidth of approximately 40 nm. To record simultaneously the spectra of different species, the C_2 and CH radicals were selected because their existence and concentration can be detected in a wavelength region between 435 and 475 nm. A number of test runs were performed during which the maximum concentrations of C_2 and CH were measured at three different cross sections along the fuel grain. It was observed that the maximum concentrations of both radicals measured showed hardly any fluctuations after termination of the ignition phase. The results are plotted in Fig. 19. It is interesting to note that the ratio measured between the CH and C_2 concentrations is fairly constant at about 10. Unfortunately, the spectroscopic technique, as was used in this setup, did not yield the exact radial location of these maximum concentrations.

Since no large fluctuations in concentrations were observed, the observed data were compared with computational results obtained by using the finite-rate chemical kinetics combustion model. Although the code predicts species concentration distributions as a function of axial and radial position, only the maximum concentrations found in every cross section along the fuel grain are plotted in Fig. 19. It is noted that the ratio between the calculated maximum CH and C_2 concentrations is also relatively constant but somewhat larger than the experimental ratio. The computational results show that, in the turbulent boundary layer, maximum concentrations occur in a thin region corresponding to the flame sheet. In the recirculation zone, however, the C_2 and CH concentrations are significant throughout this whole region. Considering the limitations of the computational model and the experimental technique, there is nevertheless good agreement between observed and predicted maximum concentrations. For a better comparison, however, the need for a more refined experimental diagnostic technique allowing for spatially resolved concentration measurements is strongly felt.

Conclusions

Experimental results obtained by burning cylindrical fuel grains made of PE have been compared with numerical data from a computer code describing the flow and combustion processes in the combustion chamber of a solid fuel ramjet. The following major conclusions are drawn:

1) In general there is a good agreement between computational and experimental results. Comparison with findings from other investigators also shows good correlation.

2) In the recirculation zone, the correlation between calculated and observed data is rather poor, which is attributed to the inability of the k-ϵ model to predict accurately the heat transfer behind a rearward facing step. Adaptation of the Chieng and Launder wall-function method needs serious consideration.

3) The importance of defining the correct value of the effective heat of gasification in relation to the test conditions is clearly revealed. Therefore, a better understanding of its behavior in relation to flow and combustion parameters is required.

4) The calculated mean regression rate is relatively insensitive to the combustion model employed.

Acknowledgments

This work has been supported by the Technology Foundation (STW) and the National Fund for Supercomputers in the Netherlands. The assistance of DLR in elucidating their experiments is gratefully acknowledged.

References

[1]Van der Geld, C. W. M., Korting, P. A. O. G., and Wijchers, T., "Combustion of PMMA, PE and PS in a Ramjet," Faculty of Aerospace Engineering, Delft Univ. of Technology, Prins Maurits Lab. TNO, Rept. LR-514, PML 1987-C18, Delft, Rijswijk, the Netherlands, April 1987.

[2]Korting, P. A. O. G., and Schöyer, H. F. R., "Experimental Connected Pipe Facility for Solid Fuel Ramjet Combustion Studies," *Proceedings of the 15th International Annual Conference of ICT,* Fraunhofer-Institut für Chemische Technologie, ICT 1984, Karlsruhe, Germany, 1984.

[3]Korting, P. A. O. G., and Schöyer, H. F. R., "A Sonic Control and Measuring Choke for the Precise Control and Measuring of Gas (Oxygen) Mass Flow Rates," Faculty of Aerospace Engineering, Delft Univ. of Technology, Prins Maurits Lab. TNO, Rept. LR-V-02, PML 1984-C59, Delft, Rijswijk, the Netherlands, 1984.

[4]Korting, P. A. O. G., and Schöyer, H. F. R., "Determination of the Regression Rate in Solid Fuel Ramjets by Means of the Ultrasonic Pulse Echo Method," *Heat Transfer in Fire and Combustion Systems*, HTD-Vol. 45, ASME, New York, 1985, pp. 347–353.

[5]Wijchers, T., "A Method for Spectroscopic Temperature Measurements in a Solid Fuel Combustion Chamber," Faculty of Aerospace Engineering, Delft Univ. of Technology, Prins Maurits Lab. TNO, Mem. M-530, PML 1985-C7, Delft, Rijswijk, the Netherlands, 1985.

[6]Aarts, W. J. A. M., and Wijchers, T., "Ontwerp van een Pyrometer ten behoeve van Temperatuurmetingen aan de Vaste Brandstof VebrandingsKamer" ("Design of a Pyrometer for Temperature Measurements on a Solid Fuel Combustion Chamber," written in Dutch), Faculty of Aerospace Engineering, Delft Univ. of Technology, Prins Maurits Lab. TNO, Rept. LR-530, PML 1987-C123, Delft, Rijswijk, the Netherlands, 1987.

[7]Vos, J. B., "The Calculation of Turbulent Reacting Flows with a Combustion Model Based on Finite Chemical Kinetics," Ph.D. Thesis, Delft Univ. of Technology, Delft, the Netherlands, April 1987.

[8]Elands, P. J. M., "The Prediction of the Flow and Combustion in a Solid Fuel Combustion Chamber by Means of Two Combustion Models Based on the Diffusion Flame Concept," AIAA Paper 87-1702, 1987.

[9]Elands, P. J. M., "The Modeling of Heat and Mass Transfer Near Solid Boundaries and Comparison with Experimental Results," Faculty of Aerospace Engineering, Delft Univ. of Technology, Prins Maurits Lab. TNO, Rept. LR-567, PML 1988-C159, Delft, Rijswijk, the Netherlands, Nov. 1988.

[10]De Wilde, J. P., "The Heat of Gasification of Polyethylene and Polymethylmethacrylate," Faculty of Aerospace Engineering, Delft Univ. of Technology, Prins Maurits Lab. TNO, Mem. LR-M-593, PML 1988-C42, Delft, Rijswijk, the Netherlands, Sept. 1988.

[11]Vos, J. B., and van Dijk, J. H., "The Development of a Computational Model for a 2-dimensional Turbulent Flow. Part II: Description of the Computer Code and Computational Results of Various Pipe Flows," Faculty of Aerospace Engineering, Delft Univ. of Technology, Prins Maurits Lab. TNO, Rept. LR-469, PML 1985-C22, Delft, Rijswijk, the Netherlands, April 1985.

[12]Milshtein, T., and Netzer, D. W., "Three-Dimensional, Primitive-Variable Model for Solid-Fuel Ramjet Combustion," *Journal of Spacecraft and Rockets*, Vol. 23, No. 1, 1986, pp. 113–117.

[13]Stevenson, C. A., and Netzer, D. W., "Primitive-Variable Model Applications to Solid-Fuel Ramjet Combustion," *Journal of Spacecraft and Rockets*, Vol. 18, No. 1, 1981, pp. 89–94.

[14]Netzer, D. W., "Modeling Solid-Fuel Ramjet Combustion," *Journal of Spacecraft and Rockets*, Vol. 14, No. 12, 1977, pp. 762–766.

[15]Netzer, A., and Gany, A., "Burning and Flameholding Characteristics of a Miniature Solid Fuel Ramjet Combustor," AIAA Paper 88-3044, 1988.

[16] Zvuloni, R., Gany, A., and Levy, Y., "Geometric Effects on the Combustion in Solid Fuel Ramjets," *Journal of Propulsion and Power*, Vol. 5, No. 1, 1989, pp. 32–37.

[17]Schulte, G., "Fuel Regression and Flame Stabilization Studies," *Journal of Propulsion and Power*, Vol. 2, No. 4, 1986, pp. 301–304.

[18]Schulte, G., Pein, R., and Högl, A., "Temperature and Concentration Measurements in a Solid Fuel Ramjet Combustion Chamber," *Journal of Propulsion and Power*, Vol. 3, No. 2, 1987, pp. 114–120.

[19]Chieng, C. C., and Launder, B. E., "On the Calculation of Turbulent Heat Transport Downstream of an Abrupt Pipe Expansion," *Momentum and Heat Transfer Processes in Recirculating Flows*, ASME 1980, HTD-Vol. 13.

[20]Patankar, S. V., *Numerical Heat Transfer and Fluid Flow*, Hemisphere, Washington, DC, 1980.

[21]Shannon, L. J., and Erickson, J. E., "Thermal Decomposition of Composite Solid Propellant Binders," *6th ICRPG Conference Expanded Abstracts and Slides*, Chemical Propulsion Information Agency, Silver Spring, MD, Pub. 192, Vol. 1, 1969, pp. 515–530.

[22]Shannon, L. J., "Composite Solid Propellant Ignition Mechanism," Air Force Office of Scientific Research, AFOSR 68-114, United Technology Center, Sunnyvale, CA (UTX 2138-FR).

[23]Fenimore, C. P., and Martin, F. J., "Burning of Polymers," *Fourth Materials Research Symposium on the Mechanisms of Pyrolysis, Oxidation and Burning of Organic Materials*, National Bureau of Standards, Washington, DC, Spec. Pub. 357, 1970, pp. 159–170.

[24]Launder, B. E., and Spalding, D. B., "The Numerical Computation of Turbulent Flows," *Computer Methods in Applied Mechanics and Engineering*, Vol. 3, North-Holland, Amsterdam, 1974, pp. 269–289.

[25]Mongia, H. C., Reynolds, R. S., and Srinivasan, R., "Multidimensional Gas Turbine Modeling: Applications and Limitations," *AIAA Journal*, Vol. 24, No. 6, 1986, pp. 890–904.

[26]Marxman, G. A., Wooldridge, C. E., and Muzzy, R. J., "Fundamentals of Hybrid Boundary Layer Combustion," *Progress in Astronautics and Aeronautics: Heterogeneous Combustion*, Vol. 15, edited by H. G. Wolfhard, I. Glassman, and L. Green, Jr., AIAA, New York, 1964, pp. 485–522.

[27]Ciofalo, M., and Collins, M. W., "k-ϵ Predictions of Heat Transfer in Turbulent Recirculating Flows Using an Improved Wall Treatment," *Numerical Heat Transfer* (submitted for publication).

[28]Phaneuf, J. T., Jr., and Netzer, D. W., "Flow Characteristics in Solid Fuel Ramjets," Naval Postgraduate School, Monterey, CA, Rept. NPS-57Nt74081, May 1974.

[29]Krall, K. M., and Sparrow, E. M., "Turbulent Heat Transfer in the Separated, Reattached, and Redevelopment Regions of a Circular Tube," *Journal of Heat Transfer, Transactions of the ASME*, Feb. 1966, pp. 131–136.